PHILOSOPHICAL MAGAZINE LETTERS, 1996, VOL. 73, NO. 4, 187–193

Liquid film migration in a Mo(Ni) bicrystal

By E. RABKIN†, D. WEYGAND†‡, B. STRAUMAL†§, V. SEMENOV§, W. GUST† and Y. BRECHET‡

†Max-Planck-Institut für Metallforschung and Institut für Metallkunde, Seestrasse 75, D-70174 Stuttgart, Germany
‡Laboratoire de Thermodynamique et Physico-chimie Métallurgiques, Ecole Nationale Supérieure d'Electrochimie et d'Electrométallergie de Grenoble, Institut National Polytechnique de Grenoble, F-38402 St Martin d'Heres, France
§Institute of Solid State Physics, Chernogolovka, Moscow District, 142432 Russia

[*Received in final form 8 January 1996 and accepted 16 January 1996*]

ABSTRACT

The liquid film migration process has been studied during the penetration of a Ni-rich liquid phase along a symmetrical 70°⟨011⟩{011} tilt grain boundary in a Mo bicrystal at 1380°C. The experimentally determined average migration rate of the film is two orders of magnitude lower than expected from an estimate made according to coherency-strain theory. This discrepancy can be explained under the assumption that the actual film migration time is much lower than the annealing time.

§ 1. INTRODUCTION

Liquid film migration (LFM) is a widely observed phenomenon in metallic systems (Baik and Yoon 1986). Liquid films occur in a material for different reasons: the melting of a eutectic phase present at the grain boundaries (GBs) (Dang and Baudelet 1994); the initial coexistence of a solid phase with a liquid phase during the material manufacture process, as during liquid-phase sintering; the interaction of a solid metal with a liquid-metal environment as in experiments on liquid-metal embrittlement (Lynch 1988); the constitutional melting of multiphase alloys during heating (Acoff, Thompson and Griffin 1994). A common condition for LFM to occur is the complete wetting of the GB by the liquid phase. If complete wetting occurs, the following condition should be valid if Herring's torque terms are neglected:

$$\gamma_{GB} > 2\gamma_{SL}, \tag{1}$$

where γ_{GB} and γ_{SL} are the excess Gibbs energies of the GB and solid–liquid interface respectively. In this case, deep narrow grooves (liquid films) along the GBs form in the polycrystalline solid embedded in a liquid-metal environment. Any small asymmetry in the properties of two solid–liquid interfaces bounding the liquid film can lead to the migration of the wetted GB in one preferred direction. This phenomenon, called LFM, has been frequently observed and is reminiscent of a similar phenomenon in the completely solid state, namely diffusion-induced grain boundary migration (DIGM) (Ma, Rabkin, Gust and Hsu 1995). However, although both phenomena are fairly ubiquitous, the origin of the driving force and the kinetics are still not completely understood. For example, most studies of LFM have been performed on powders undergoing sintering with a liquid phase. The geometry of the

liquid film in such a situation is governed by the geometry of the contacts between the grains in the powder and cannot be controlled during the experiment.

In the present study, we have chosen a system which has already been investigated by sintering experiments, but we perform better controlled experiments using a bicrystal. Figure 1 (*a*) shows the geometry of our experimental set-up; a layer of the low melting point metal (Ni) is deposited on the external surface of a Mo bicrystal. The Mo–Ni system was chosen because LFM can easily be observed in the systems Mo–Ni–Fe (Baik and Yoon 1986), Mo–Ni–Co–Sn (Rhee and Yoon 1987) and Mo–W–Ni (Lee and Yoon 1992). It has been shown in sintering experiments that the LFM velocity scales with δ^2, where δ is the coherency strain arising from the addition of a ternary element (Rhee and Yoon 1987). It was suggested for this system that the elastic energy due to the misfit associated with the gradient in the Ni concentration ahead of the moving film is the driving force for LFM. In particular, it was shown that, when the misfit was exactly compensated by ternary alloying, LFM did not occur. This indicates that the chemical contribution to the driving force for LFM in this system is below the threshold for migration (Brechet and Purdy 1989). This well defined system is therefore an ideal candidate for well controlled experiments on bicrystals where the misorientation between the grains, the thickness of the liquid film, and the velocity of LFM can be readily observed.

§ 2. Experimental details

A Mo bicrystal with a symmetrical $\langle 011\rangle\{011\}$ tilt GB having a misorientation angle $\phi = 70°$ has been used. This bicrystal was grown using the electron-beam floating-zone method. A Ni layer was deposited on the bicrystal surface and the specimen was annealed in a vacuum of 3×10^{-4} Pa at 1380°C for 20 min. This temperature lies slightly above the peritectic temperature of the Mo–Ni system (1362°C), but still below the melting temperature of pure Ni (Massalski *et al.*

Fig. 1

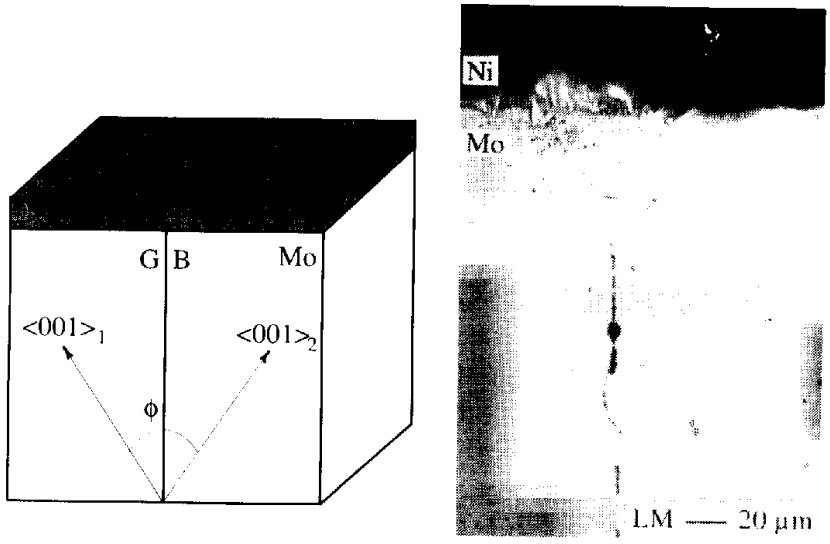

(*a*) (*b*)

(*a*) Preparation scheme of the Mo bicrystal used for the experiment. (*b*) Optical micrograph of the specimen cross-section after annealing at 1380°C for 20 min.

1990), so that the liquid phase forms at the Mo–Ni interface during the anneal. This liquid phase, containing about 60 at.% Ni (Massalski *et al.* 1990), wets the GB completely and spreads along it, forming a liquid film. The morphology and position of this film were observed by optical microscopy on a cross-section prepared by standard metallographic methods. The concentration of Ni in the alloy was measured by electron probe microanalysis (EPMA). The intensity of the Ni Kα line was measured with the aid of a wave-dispersive spectrometer, and conventional software for quantitative analysis was used.

§ 3. Results and discussion

In fig. 1 (*b*) an optical micrograph of a Mo bicrystal is shown after the annealing in contact with Ni at 1380°C. The following features can be seen on this micrograph:

(1) a GB groove near the surface of the bicrystal, having the characteristic form of the groove resulting from the penetration of the liquid metal along the GB;
(2) a film along the GB having an optical contrast different from the bulk of Mo;
(3) a curve region of the GB film, which resembles the typical morphologies of DIGM and LFM.

EPMA measurements of the Ni concentration have been performed in order to quantify these features. The Ni concentration inside the GB groove near the surface of the bicrystal is about 47 at.%. This corresponds to the MoNi intermetallic phase, which is stable up to 1362°C. According to the Mo–Ni equilibrium phase diagram, the MoNi phase forms during cooling of the sample as the result of a peritectic reaction between the Ni-rich melt and Mo (Massalski *et al.* 1990). Therefore the liquid phase was present in our sample during the anneal. In fig. 2 (*a*), a contour plot is shown of the Ni distribution in two dimensions in the curved region obtained by EPMA measurements. The position of the film visible in the micrograph (fig. 1 (*b*)) is connected with the Ni concentration spike, which can be as high as 12 at.%. Of course, this does not mean that this is the actual Ni concentration of the film phase. Indeed, the zone in the sample excited by the electron beam during the EPMA measurement is approximately 2 μm in diameter. If the electron beam is positioned in the middle of the film, then the following approximate relationship between the actual Ni concentration C_F in the film and the measured concentration C_m should be valid:

$$c_m = \frac{2d}{\pi r} c_F, \tag{2}$$

where d and r are the film width and the radius respectively of the zone excited by the electron beam. Substituting $c_F = 47$ at.% (the Ni concentration in the solidification product of the Ni-rich liquid phase), $c_m = 12$ at.%, and $r = 1$ μm we get, from eqn. (2), $d \approx 0{\cdot}4$ μm, which is close to the film width, which could be estimated from the optical micrograph in fig. 1 (*b*)). Therefore the curved region in fig. 1 (*b*) corresponds to a liquid film approximately 0·4 μm wide at the GB, which migrated during the experiment, and we are dealing with the typical LFM phenomenon. As can be seen from fig. 2 (*a*), the Ni concentration profile across the liquid film is asymmetric, the Ni content in the alloyed zone left behind the migrating film being about 1·5 at.%, which corresponds approximately to the solubility of Ni in Mo at 1380°C. The

Fig. 2

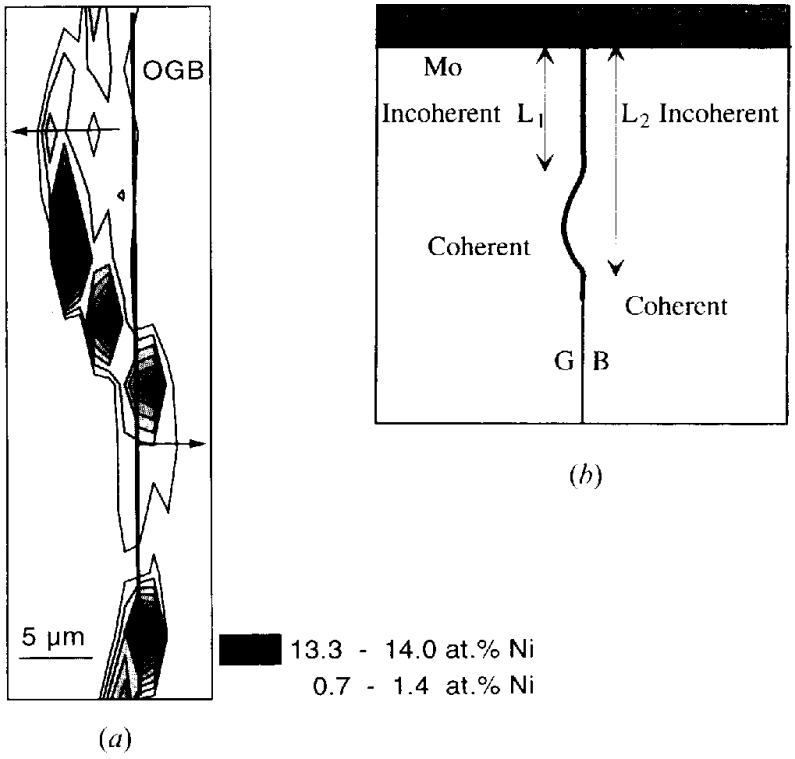

(*a*) Contour plot of the Ni distribution in the LFM zone. The directions of film migration are shown by the arrows. The original position of the grain boundary (OGB) is shown. (*b*) Schematic illustration showing the development of incoherent zones along the liquid film. The LFM phenomenon occurs at those sections of the liquid film at which the coherency is lost only from one side.

characteristic S-type LFM morphology (migration in both directions) can be also seen in fig. 2 (*a*), although it is not so obvious from the LFM micrograph (fig. 1 (*b*)). The Ni is not homogeneously distributed along the final GB or liquid film position; it seems to be collected in droplets distributed along the GB. Such a 'string-of-pearls' morphology has been observed in other systems during the rapid penetration of a liquid phase along GBs (Vogel and Ratke 1991).

The migration distance measured from figs. 1 (*b*) and 2 (*a*) is 6 μm in 20 min. The migration rate v is assumed to be constant during the heat treatment: $v \approx 5\,\mathrm{nm\,s^{-1}}$. This is in accordance with data from the literature (Song, Ahn and Yoon 1985). The bulk diffusion coefficient of Ni in Mo at 1350°C lies between $2{\cdot}4 \times 10^{-16}$ and $3{\cdot}2 \times 10^{-16}\,\mathrm{m^2\,s^{-1}}$ (Mehrer 1990). We shall take the value of $3 \times 10^{-16}\,\mathrm{m^2\,s^{-1}}$ (Mehrer 1990). We shall take the value of $3 \times 10^{-16}\,\mathrm{m^2\,s^{-1}}$ at 1380°C to make estimates. This corresponds for a 20 min anneal to an average width of the bulk diffusion zone of 0·6 μm. This width is large enough to dissipate the chemical driving force for LFM. Therefore, the coherency-strain model should be relevant, and we can use this model for an estimation of the velocity of the liquid film. If only the grain ahead of the migrating film is elastically stressed, the Gibbs energy difference ΔG across the film is given by

$$\Delta G = Y\delta^2, \tag{3}$$

where $\delta = \eta(c_S^{Ni,0} - c_S^{Ni})$, η being the lattice misfit parameter $\eta = -0{\cdot}054$ for Ni–Mo (Rhee and Yoon 1987), c_S^{Ni} and $c_S^{Ni,0}$ are the Ni concentrations at the solid–liquid interface and far from the liquid film in the bulk of Mo respectively. In the present study, $c_S^{Ni} \approx 0{\cdot}015$ and $c_S^{Ni,0} = 0$. Y is an elastic parameter dependent on the interface normal, which can be calculated according to the method of Hilliard (1970). The velocity of the liquid film is then (Handwerker 1988)

$$\nu = \frac{D_L V_m c_L(1 - c_L)}{RTd(c_L - c_S^{Ni})^2} \Delta G, \tag{4}$$

where D_L, V_m, c_L, R and T are the diffusion coefficient in the liquid, the molar volume of the liquid phase, the liquidus concentration, the gas constant and the absolute temperature respectively. For the calculation of Y at 1380° in the direction of the GB normal **n**, given by the expression

$$\mathbf{n} = \begin{bmatrix} l \\ m \\ n \end{bmatrix} = \begin{bmatrix} \frac{1}{2^{1/2}} \cos\left(\frac{\phi}{2}\right) \\ -\frac{1}{2^{1/2}} \cos\left(\frac{\phi}{2}\right) \\ -\sin\left(\frac{\phi}{2}\right) \end{bmatrix} \tag{5}$$

with respect to the standard axes, where $\phi = 70°$, the values of the elastic constants at 1380° were estimated using the measured temperature dependence between −200 and 700°C (Dickinson and Armstrong 1967). We obtained, for 1380°C, $c_{11} = 372\,\text{GPa}$, $c_{12} = 164\,\text{GPa}$ and $c_{44} = 93{\cdot}3\,\text{GPa}$. The calculated elastic constant is $Y = 365\,\text{GPa}$. Then, from eqns. (3)–(5), using the characteristic for the liquid-phase value of the diffusion coefficient $D_L \approx 3 \times 10^{-9}\,\text{m}^2\,\text{s}^{-1}$ and $d = 0{\cdot}4\,\mu\text{m}$, we find that the liquid-film velocity that we observe is two orders of magnitude smaller than the value predicted according to the coherency-strain model. This discrepancy cannot come from neglecting the chemical contribution to the driving force. Another possible reason for it is neglect of the contribution to ΔG arising from the curvature of the liquid film, which slows down the film motion. This contribution changes the driving force for LFM:

$$\Delta G = Y\delta^2 - \frac{2\gamma_{SL}}{a}, \tag{6}$$

where a is the radius of curvature of the film. As a rough estimate of γ_{SL} for the solid Mo–liquid Mo–Ni alloy, we take the excess energy of the solid–liquid interface in pure Mo, $500\,\text{mJ}\,\text{m}^{-2}$ (Miedema and den Broeder 1979). From the micrograph in fig. 1 (*b*), $a \approx 20\,\mu\text{m}$, which gives a negligibly small correction to the coherency-strain driving force. However, at the early stage of the LFM process, the bulge could be very small and retard the film migration considerably. Taking into account the relationship $\nu = \text{d}a/\text{d}t$, where t is the time, one can obtain from eqns. (4) and (6) a differential equation for a which has the following solution:

$$a - a_0 + a_c \ln\left(\frac{a - a_c}{a_0 - a_c}\right) = \frac{D_L V_m c_L(1 - c_L)}{RTd(c_L - c_S^{Ni})^2} Y\delta^2 t, \tag{7}$$

where $a_c = 2\gamma_{SL}/Y\delta^2$ and a_0 is the bulge radius at $t = 0$. Only bulges with $a_0 > a_c$ can grow under the action of the coherency-strain driving force. For the Mo(Ni) system, $a_c \approx 4{\cdot}2\,\mu\text{m}$, which excludes the possibility of formation of the critical LFM nucleus by thermal fluctuations (this is similar to the problem of nucleation of recrystallization (Humphreys and Hatherly 1995)). Therefore, the LFM process

can start only from a pre-existing bulge of the radius $a_0 > a_c$, or it can develop by some other mechanism. The logarithmic term on the left-hand side of eqn. (7) is very insensitive to the value of a_0. For example, for $a_0 = 4{\cdot}201\,\mu m$ (which exceeds the a_c value by only 1 nm) the bulge radius after 20 min annealing should be 537 μm according to eqn. (7), which is still about two orders of magnitude higher than the experimentally observed liquid film displacement. Therefore the influence of the film curvature cannot explain the observed discrepancy.

In our opinion, the two most probable reasons for the discrepancy between theory and experiment are as follows.

(1) The LFM process in Mo–Ni is not diffusion controlled but interface controlled. It is known that, in a number of metallic systems, the precipitate dissolution and constitutional melting are interface controlled (Radhakrishnan 1993). In this case, eqn. (3) should be replaced by the general relationship $v = M\,\Delta G$, where M is the mobility of the liquid film, which can be very small.

(2) The liquid film has migrated not during the whole annealing time of 20 min, but during a shorter period of time. Then the actual (instantaneous) film velocity is higher than the estimated average value of $5\,nm\,s^{-1}$.

We now consider possibility (2) in more detail. In our experiment, the Ni-rich liquid film penetrates along the GB from the surface of the sample into the interior of the bicrystal. Then Ni diffuses from the liquid phase in the film into the two grains, which causes coherency strains in them. The coherency-strain energy increases as the bulk diffusion of Ni proceeds, and at some moment the transition from a coherent to an incoherent Ni-rich layer occurs. If the loss of coherency occurs simultaneously in both grains of the bicrystal, no LFM would occur. For the LFM it is important that the incoherent Ni-rich layer in one grain is in advance of such a layer in the other grain (see fig. 2(*b*)). However, both incoherent layers spread downwards together with the liquid film to the bicrystal interior. When the 'retarded' incoherent layer catches up with the advanced layer, the LFM process stops. The time Δt, during which the LFM process occurred, can be estimated as follows. We assume that the liquid film penetrates into the Mo bicrystal according to the parabolic law $L = A/t^{1/2}$ where L and A are the penetration depth and a time-independent constant respectively. Under the assumptions that the left incoherent layer stops for some reason and then catches up with the right layer instantly, and that the spreading rate of the incoherent layer follows the same kinetic law as that of the liquid film, $\Delta t = (L_2/A)^2 - (L_1/A)^2$, where L_1 and L_2 are defined in fig. 2(*b*). From fig. 1(*b*), $L_1 \approx 134\,\mu m$ and $L_2 \approx 165\,\mu m$. A can be estimated from the overall spreading kinetics: the 'strings-of-pearls' morphology is visible on the micrographs up to $L \approx 1\,mm$ after a 20 min anneal. Therefore $A \approx 2{\cdot}9 \times 10^{-5}\,m\,s^{1/2}$. Then $\Delta t \approx 11\,s$, which means that the actual film velocity was $0{\cdot}5\,\mu m\,s^{-1}$. This value resolves the discrepancy between theory and experiment. The difference of up to three orders of magnitude between the instantaneous and averaged GB velocities is also characteristic of the discontinuous precipitation reaction (Kaur, Mishin and Gust 1995). It should be noted that, according to the EPMA data (fig. 2(*a*)), backward LFM under the action of the film curvature did not occur, which means that this driving force is below the threshold for the LFM process.

In conclusion, our experimental results can be made consistent with the coherency-strain model for LFM only under the assumption that the actual migration

time is about two orders of magnitude lower than the annealing time, or that the LFM process is not diffusion controlled but interface controlled.

ACKNOWLEDGMENTS

The authors like to thank Professor Shvindlerman and Dr Sursaeva for stimulating discussions. Financial support of the International Science Foundation (under Grant No. RER300) is heartily acknowledged.

REFERENCES

ACOFF, V. L., THOMPSON, R. G., and GRIFFIN, R. D., 1994, *Solid–Solid Phase Transformations*, edited by W. C. Johnson, J. M. Howe, D. E. Laughlin and W. A. Soffa (Warrendale, Pennsylvania: Metallurgical Society of AIME), p. 1207.

BAIK, Y.-J., and YOON, D. N., 1986, *Acta metall.*, **34**, 2039.

BRECHET, Y. J. M., and PURDY, G. R., 1989, *Acta metall.*, **37**, 2253.

DANG, M. C., and BAUDELET, B., 1994, *J. Mater. Sci.*, **29**, 2315.

DICKINSON, J., and ARMSTRONG, P., 1967, *J. appl. phys.*, **38**, 602.

HANDWERKER, C. A., 1988, *Diffusion Phenomena in Thin Films and Microelectronic Materials*, edited by D. Gupta and P. Ho (Park Ridge, New Jersey: Noyes), p. 245.

HILLIARD, J. E., 1970, *Phase Transformations*, edited by H. I. Aaronson (Metals Park, Ohio: American Society for Metals), p. 497.

HUMPHREYS, F. J., and HATHERLY, M., 1995, *Recrystallization and Related Annealing Phenomena* (Oxford: Elsevier), p. 207.

KAUER, I., MISHIN, Y., and GUST, W., 1995, *Fundamentals of Grain and Interphase Boundary Diffusion* (Chichester, West Sussex: Wiley), p. 318.

LEE, K.-R., and YOON, D. N., 1992, *Acta metall. mater.*, **40**, 107.

LYNCH, S. P., 1988, *Acta metall.*, **36**, 2639.

MA, C. Y., RABKIN, E., GUST, W., and HSU, S. E., 1995, *Acta metall. mater.*, **43**, 3113.

MASSALSKI, T. B., OKAMOTO, H., SUBRAMANIAN, P. R. and KACPRZAK, L. (editors), 1990, *Binary Alloy Phase Diagrams* (Materials Park, Ohio: American Society for Metals), p. 2635.

MEHRER, H. (editor), 1990, *Diffusion in Solid Metals and Alloys*, Landolt Börnstein New Series, Group III, Vol. 26 (Berlin: Springer), p. 120.

MIEDEMA, A. R., and DEN BROEDER, F. J. A., 1979, *Z. Metallk*, **70**, 14.

RADHAKRISHNAN, B., 1993, *Int. Sci.*, **1**, 175.

RHEE, W.-H., and YOON, D. N., 1987, *Acta metall.*, **35**, 1447.

SONG, Y.-D., AHN, S.-T., and YOON, D. N., 1985, *Acta metall.*, **33**, 1907.

VOGEL, H. J., and RATKE, L., 1991, *Acta metall. mater.*, **39**, 641.